

Supporting Information for

Density functional theory prediction of Mg_3N_2 as a high-performance anode material for Li-ion batteries

Lixin Xiong¹, Junping Hu^{2*}, Sicheng Yu¹, Musheng Wu¹, Bo Xu¹, Chuying Ouyang^{1*}

¹Department of Physics, Laboratory of Computational Materials Physics, Jiangxi Normal University, Nanchang, 330022, China

²School of Science, Nanchang Institute of Technology, Nanchang 330099, China

*Corresponding author's E-mail: jphu@nit.edu.cn

*Corresponding author's E-mail: cyouyang@jxnu.edu.cn

SI-1. Concentration dependent Li-ion adsorption energy

Table S1. The concentration dependent Li-ion adsorption energies (in eV) at the bridge sites calculated with different supercell sizes. The supercells in this table are created using the orthogonal supercell as the unitcell.

supercells	1×1	1×2	2×2	1×3	2×3	3×3
E_{ad} (eV)	-2.36	-2.45	-2.48	-2.47	-2.52	-2.53

SI-2. Hybrid functional tests

It is known that PBE calculations always underestimate the band gap of insulating (semiconducting) materials. In order to test the reliability of the PBE results, we calculated the electronic band structure of the pristine and lithiated g- Mg_3N_2 with hybrid functional (HSE06) [1]. We selected two Li concentrations to test our results, namely, $\text{Li}_1\text{Mg}_3\text{N}_2$ (small Li concentration) and $\text{Li}_7\text{Mg}_3\text{N}_2$ (fully lithiated state). **Figure S1** presents the electronic band structures of the g- Mg_3N_2 and its partially and fully lithiated states from HSE06 calculations.

With the above HSE06 data, we also evaluated the average intercalation potentials, which are given in the following **Table S2**, with comparing data of the results from PBE calculation.

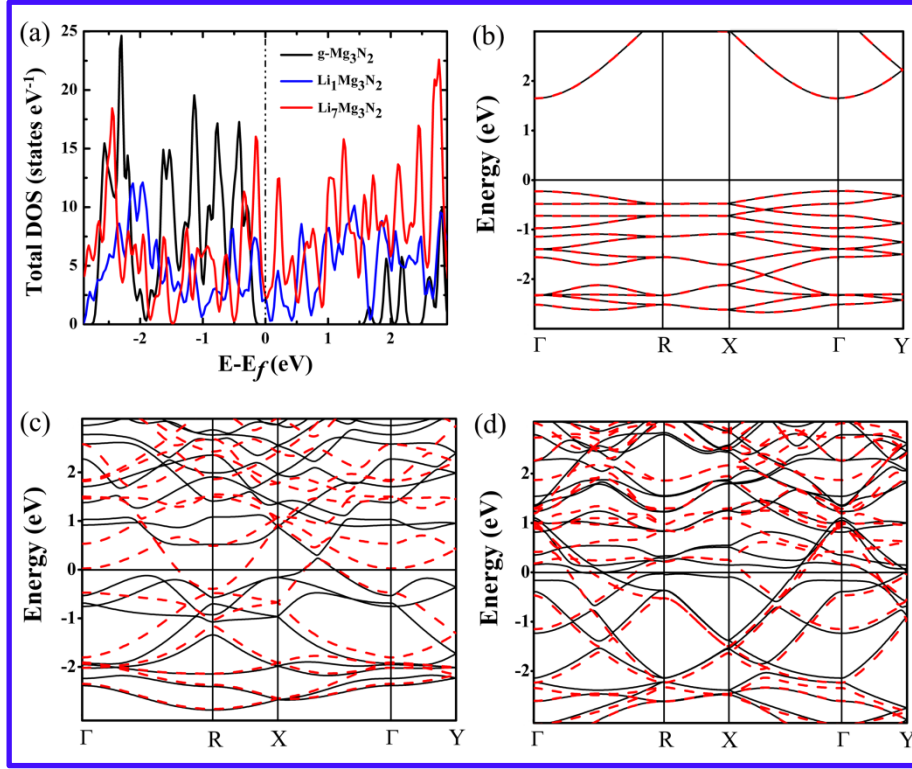


Fig. S1. (a) The total DOS of the $g\text{-Mg}_3\text{N}_2$ and its partially and fully lithiated states calculated from HSE06. The Fermi level is aligned to 0 eV. (b)-(d) are the electronic band structures of $\text{Li}_x\text{Mg}_3\text{N}_2$ with $x=0, 1$ and 7 , respectively. The black solid and red dashed lines are for spin-up and spin-down, respectively.

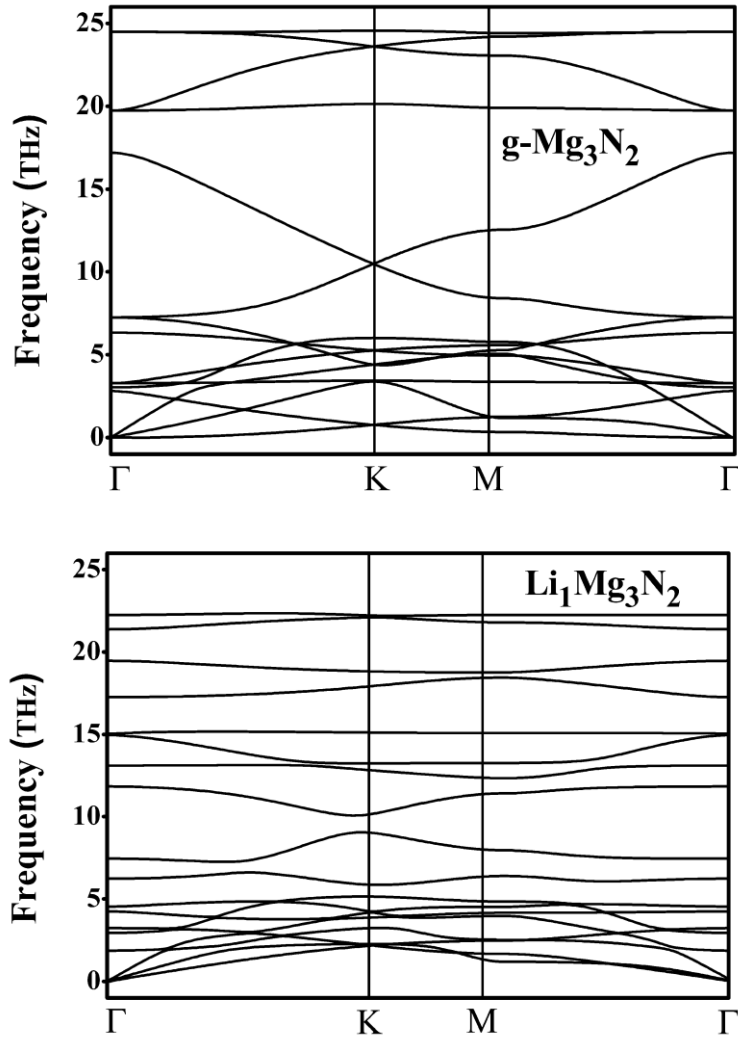
Table S2. Average intercalation potentials (in V) of $\text{Li}_1\text{Mg}_3\text{N}_2$ and $\text{Li}_7\text{Mg}_3\text{N}_2$ calculated from PBE and HSE06.

	PBE	HSE06
$\text{Li}_1\text{Mg}_3\text{N}_2$	0.65	0.67
$\text{Li}_7\text{Mg}_3\text{N}_2$	0.34	0.35

SI-3. Phonon dispersion data of the $g\text{-Mg}_3\text{N}_2$ and its lithiated states.

The vibrational calculations are performed using linear response method, and the phonon data is collected with the PHONONPY code [2]. The results are presented in Fig. S2. As is seen, no imaginary frequencies are observed for the case of $g\text{-Mg}_3\text{N}_2$ and $\text{Li}_1\text{Mg}_3\text{N}_2$, indicating that the structures of them are dynamically stable. However,

very small imaginary frequencies are observed in the phonon dispersion spectrum of the $\text{Li}_7\text{Mg}_3\text{N}_2$, as marked with red arrow in Fig. S3. The detailed vibrational frequencies are also presented in the following. Although small imaginary frequencies (0.00215 THz or 0.07 cm^{-1}) are observed near the Γ -point, we still believe that the structure of the $\text{Li}_7\text{Mg}_3\text{N}_2$ is dynamically stable, because it is generally accepted that these small imaginary frequencies (small than 1 cm^{-1}) could be an artifact of the simulation or lattice instabilities corresponding to long wave undulations [3, 4], which were also found in other dynamically stable 2D materials. These imaginary frequencies can be removed through technique treatments like increasing the accuracy of the calculation or using different calculation methods.



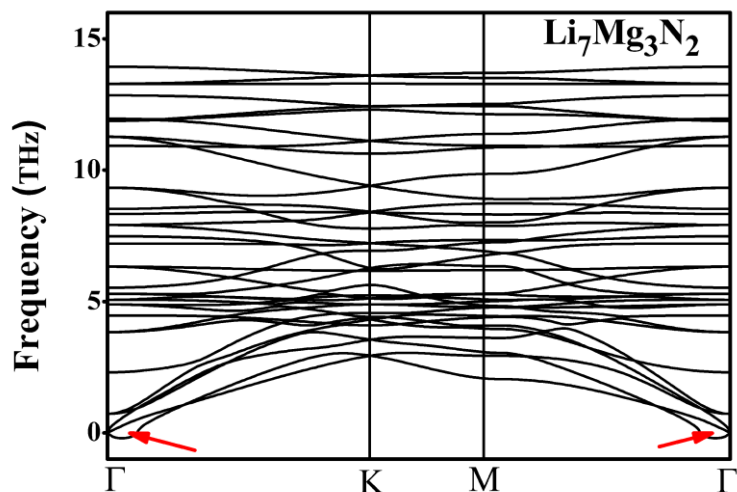


Fig. S2. The phonon dispersion spectrum of g-Mg₃N₂, Li₁Mg₃N₂ and Li₇Mg₃N₂.

Vibrational frequencies of the Li₇Mg₃N₂

1 f =	13.863368 THz	87.106108 2PiTHz	462.432156 cm-1	57.334301 meV
2 f =	13.223850 THz	83.087899 2PiTHz	441.100138 cm-1	54.689467 meV
3 f =	13.223850 THz	83.087899 2PiTHz	441.100138 cm-1	54.689467 meV
4 f =	12.554240 THz	78.880617 2PiTHz	418.764362 cm-1	51.920182 meV
5 f =	11.723368 THz	73.660094 2PiTHz	391.049454 cm-1	48.483970 meV
6 f =	11.619928 THz	73.010163 2PiTHz	387.599078 cm-1	48.056178 meV
7 f =	11.619928 THz	73.010163 2PiTHz	387.599078 cm-1	48.056178 meV
8 f =	11.113061 THz	69.825419 2PiTHz	370.691788 cm-1	45.959941 meV
9 f =	11.113061 THz	69.825419 2PiTHz	370.691788 cm-1	45.959941 meV
10 f =	10.810559 THz	67.924746 2PiTHz	360.601427 cm-1	44.708895 meV
11 f =	9.151041 THz	57.497684 2PiTHz	305.245847 cm-1	37.845675 meV
12 f =	9.151041 THz	57.497684 2PiTHz	305.245847 cm-1	37.845675 meV
13 f =	8.449508 THz	53.089822 2PiTHz	281.845229 cm-1	34.944367 meV
14 f =	8.295231 THz	52.120472 2PiTHz	276.699106 cm-1	34.306329 meV
15 f =	7.744114 THz	48.657704 2PiTHz	258.315835 cm-1	32.027093 meV
16 f =	7.744114 THz	48.657704 2PiTHz	258.315835 cm-1	32.027093 meV
17 f =	7.415315 THz	46.591800 2PiTHz	247.348287 cm-1	30.667290 meV
18 f =	7.199766 THz	45.237462 2PiTHz	240.158324 cm-1	29.775848 meV
19 f =	6.243821 THz	39.231084 2PiTHz	208.271441 cm-1	25.822377 meV
20 f =	6.243821 THz	39.231084 2PiTHz	208.271441 cm-1	25.822377 meV
21 f =	5.496925 THz	34.538197 2PiTHz	183.357666 cm-1	22.733461 meV
22 f =	5.141950 THz	32.307825 2PiTHz	171.516987 cm-1	21.265404 meV
23 f =	5.141950 THz	32.307825 2PiTHz	171.516987 cm-1	21.265404 meV
24 f =	4.959203 THz	31.159591 2PiTHz	165.421200 cm-1	20.509622 meV
25 f =	4.959203 THz	31.159591 2PiTHz	165.421200 cm-1	20.509622 meV
26 f =	4.787436 THz	30.080348 2PiTHz	159.691675 cm-1	19.799251 meV

27 f =	4.787436 THz	30.080348 2PiTHz	159.691675 cm-1	19.799251 meV
28 f =	4.348101 THz	27.319925 2PiTHz	145.037037 cm-1	17.982307 meV
29 f =	3.796124 THz	23.851750 2PiTHz	126.625060 cm-1	15.699512 meV
30 f =	3.796124 THz	23.851750 2PiTHz	126.625060 cm-1	15.699512 meV
31 f =	2.283780 THz	14.349413 2PiTHz	76.178699 cm-1	9.444958 meV
32 f =	0.787947 THz	4.950816 2PiTHz	26.283079 cm-1	3.258688 meV
33 f =	0.787947 THz	4.950816 2PiTHz	26.283079 cm-1	3.258688 meV
34 f/i =	0.001309 THz	0.008224 2PiTHz	0.043662 cm-1	0.005413 meV
35 f/i =	0.002150 THz	0.013510 2PiTHz	0.071720 cm-1	0.008892 meV
36 f/i =	0.002150 THz	0.013510 2PiTHz	0.071720 cm-1	0.008892 meV

References:

- [1] Krukau, A. V.; Vydrov, O. A.; Izmaylov A. F.; and Scuseria, G. E.; Influence of the exchange screening parameter on the performance of screened hybrid functionals. *J. Chem. Phys.*, **2006**, 125, 224106.
- [2] Togo, A.; Tanaka, I. First principles phonon calculations in materials science. *Scr. Mater.* **2015**, 108, 1-5.
- [3] Shao, Y. F.; Shao, M. M.; Kawazoe., Y.; Shi, X. Q.; Pan, H.; Exploring new two-dimensional monolayers: pentagonal transition metal borides/carbides (penta-TMB/Cs), *J. Mater. Chem. A*, **2018**, 6, 10226-10232.
- [4] S. Cahangirov, M. Topsakal, E. Aktürk, H. Şahin and S. Ciraci, Two- and one-dimensional honeycomb structures of silicon and germanium, *Phys. Rev. Lett.*, **2009**, 102, 236804.